https://doi.org/10.5194/egusphere-2026-4195
Preprint. Discussion started: 17 August 2026

Luminescence Dating Reveals Multiple Late Quaternary Eruptions at the Soda Lake Volcanic Center, Nevada

Kathleen Rodrigues[1], Philipp P. Ruprecht[2], Craig M. de Polo[3]

[1]Division of Earth and Ecosystem Sciences, Desert Research Institute, Reno, NV, 89512, USA
[2]Department of Geological Sciences and Engineering, University of Nevada, Reno, Reno, NV, 89557, USA
[3]Nevada Bureau of Mines and Geology, University of Nevada, Reno, Reno, NV, 89557, USA

Correspondence to: Kathleen Rodrigues (Kathleen.Rodrigues@dri.edu)

Abstract. The Soda Lake volcanic center in western Nevada is the youngest known volcanic system in the state, yet its eruptive history remains poorly constrained because of conflicting stratigraphic interpretations and the limitations of conventional radiometric dating in young mafic volcanic terrains. Here we apply post-infrared infrared stimulated luminescence (post-IRIR) dating to potassium-rich feldspar separates extracted from volcaniclastic sediments and plagioclase phenocrysts extracted from juvenile basalt bombs to directly constrain the timing of eruptive activity using two distinct luminescence resetting pathways: complex eruption- and transport-related resetting of volcaniclastic grains (including variable thermal, optical, and mechanical resetting) and thermal resetting of feldspar phenocrysts within basalt bombs. Single-grain post-IRIR measurements of surge and reworked volcaniclastic deposits indicate eruptions at ~5.5 ka and ~12.5 ka. The ~5.5 ka eruption is further corroborated by plagioclase phenocrysts extracted from basalt bombs associated with the youngest eruptive phase, which yielded statistically indistinguishable ages. Despite contrasting depositional histories and luminescence resetting mechanisms, ages derived from sedimentary and bomb-derived materials are internally consistent, demonstrating that reliable eruption chronologies can be established from multiple components of a volcanic system. More broadly, the results demonstrate that eruption-related luminescence resetting may be preserved in juvenile phenocrysts, volcaniclastic sediments, and potentially xenocrystic materials, substantially expanding the range of datable components available in young mafic volcanic systems. These results resolve long-standing uncertainties regarding the eruptive history of the Soda Lake volcanic center and demonstrate the broader potential of luminescence dating for directly constraining young basaltic volcanism in settings where conventional geochronologic methods are ineffective.

1 Introduction

The Soda Lake volcanic center in western Nevada provides an ideal setting in which to evaluate these approaches. Two maar craters exist—Big Soda Lake and Little Soda Lake—together with associated tuff rings and pyroclastic deposits composed of juvenile basalt bombs, and abundant lithic material entrained during eruption (Louie and Ruprecht, 2021; Morrison, 1964; Russell, 1885). The maars lie within the Lahontan Basin of the Basin and Range Province, where Quaternary volcanism has been influenced by regional extension, transtensional deformation associated with the Pacific-North American

https://doi.org/10.5194/egusphere-2026-4195
Preprint. Discussion started: 17 August 2026

plate boundary, and fluctuating groundwater conditions favorable for phreatomagmatic activity (Bennett et al., 2003; Faulds et al., 2005; Oldow and Craig, 1992).

Despite the youthful morphology and excellent preservation of volcanic deposits at the Soda Lake volcanic center, the timing of eruptive activity remains poorly constrained. Attempts to apply $^{40}Ar/^{39}Ar$ dating to eruptive products have been unsuccessful because of insufficient radiogenic Ar accumulation (J. Price, pers. comm., 2022). Existing chronologic interpretations therefore rely primarily on indirect evidence, including stratigraphic relationships with Lake Lahontan deposits and radiocarbon measurements from lacustrine sediments recovered within Big Soda Lake (Adams et al., 2008; Rosen et al., 2021). However, many of these radiocarbon ages are stratigraphically inconsistent and likely reflect sediment disturbance, slumping, and reworking within the maar basin. Resolving the eruptive chronology is important not only for reconstructing the evolution of the Soda Lake volcanic center, but also for evaluating the recurrence of Quaternary volcanism in the northern Walker Lane and improving volcanic hazard assessments in the western Great Basin. These uncertainties highlight the need for geochronologic approaches capable of directly constraining eruption timing using materials intrinsic to the volcanic system itself.

Young mafic volcanic systems represent a persistent geochronologic challenge because conventional radiometric approaches are often difficult to apply to basaltic eruptions characterized by low potassium concentrations and limited radiogenic ingrowth (McDougall and Harrison, 1999). As a result, eruption chronologies for many late Quaternary basaltic volcanic fields remain poorly constrained despite excellent geomorphic preservation. Several approaches have been used to establish chronologies for young (e.g., Holocene) volcanic eruptions. Radiocarbon dating of charred vegetation, paleosols, peat, or lacustrine sediments associated with volcanic deposits is among the most widely applied methods but commonly provides only minimum or maximum limiting ages and may be affected by reworking or contamination (e.g., Madeira et al., 1995; Sun et al., 2019; Zaretskaya et al., 2007). Cosmogenic nuclide exposure dating has also been applied to young lava flows and volcanic landforms, although its precision is often limited for Holocene surfaces by low nuclide inventories and uncertainties associated with inheritance and erosion (e.g., Foeken et al., 2009; Heineke et al., 2016). Stratigraphic relationships have also been widely used to constrain the timing of Holocene volcanism by relating volcanic deposits to independently dated sedimentary sequences or geomorphic features (e.g., Adams et al., 2008; Morrison, 1964; Russell, 1885). Although these approaches can provide valuable chronological constraints, they generally yield only relative or limiting ages and depend on the preservation and correct interpretation of the stratigraphic record.

Luminescence dating provides an alternative approach for constraining eruption ages because volcanic processes can directly reset trapped-charge signals in silicate mineral grains through heating, sunlight exposure, and mechanical stress. As a result, volcanic and volcaniclastic materials may preserve datable luminescence signals directly related to eruption timing. Importantly, eruption-related resetting may occur in both juvenile mineral phases and entrained xenocrystic or lithic material, thereby substantially expanding the range of datable components available in young mafic volcanic systems where conventional radiometric chronometers are often absent or poorly resolved. Recent studies have demonstrated the successful

https://doi.org/10.5194/egusphere-2026-4195
Preprint. Discussion started: 17 August 2026

application of luminescence dating to young volcanic eruptions (e.g. Schmidt et al., 2017a, b), highlighting its potential for directly constraining eruption chronologies while also illustrating the challenges posed by heterogeneous signal resetting.

Methodological developments, particularly post-infrared infrared stimulated luminescence (post-IRIR; Buylaert et al., 2009 and Thomsen et al., 2008) protocols and single-grain measurement approaches, have substantially improved the reliability of feldspar luminescence dating in partially bleached sediments, where grains may not have experienced complete signal resetting of the light-sensitive luminescence signal prior to burial (Smedley et al., 2019). These advances are especially important in phreatomagmatic volcanic systems, where eruption and depositional processes can produce heterogeneous resetting histories within volcaniclastic deposits. Feldspar is particularly well suited for such applications because it may be present both as phenocrysts within juvenile volcanic products and as detrital grains within volcaniclastic sediments, thereby preserving multiple independent records of eruption-related resetting. Recent work by (Rufer et al., 2012) further demonstrated that thermally reset xenocrystic quartz- and feldspar-bearing clasts incorporated into eruptive products may preserve eruption ages, highlighting the broader potential of luminescence methods for directly dating volcanic systems using both juvenile and externally derived materials.

Here we apply post-IRIR dating to volcaniclastic sediments and juvenile basalt bombs associated with the Soda Lake volcanic center to directly constrain the timing of eruptive activity. We combine single-grain post-IRIR$_{150}$ measurements of potassium-rich feldspar grains (measured at 150 °C following a low-temperature [50 °C] IR stimulation) isolated from volcaniclastic deposits with multigrain post-IRIR$_{225}$ analyses of plagioclase phenocrysts extracted from juvenile basalt bombs. These two sample types likely experienced fundamentally different luminescence resetting environments, with volcaniclastic sediments potentially reset through varying combinations of optical, thermal, and mechanical processes during eruption, whereas the juvenile basalt bombs were reset through high-temperature magmatic processes.

By integrating luminescence chronologies with volcanic stratigraphy and regional paleohydrologic constraints, we refine the eruptive history of the Soda Lake volcanic center and demonstrate the broader applicability of luminescence methods for dating young mafic volcanic systems, where conventional geochronologic techniques commonly produce uncertainties on the order of the eruption ages themselves, thereby limiting development of high-resolution eruptive chronologies. Importantly, the study evaluates eruption chronology using materials characterized by fundamentally different luminescence resetting pathways, providing an opportunity to assess the consistency of independent eruption-age archives within the same volcanic system.

2 Study area and stratigraphic context

The Soda Lake volcanic center is a late Quaternary basaltic eruptive system located in northwestern Nevada within the Lahontan Basin, approximately 90 km east of Reno (39°31’30.78” N, 118°52’39.08” W) and comprises two closely spaced maar craters—Big Soda Lake and Little Soda Lake—together with associated tuff rings and pyroclastic deposits (Figure 1). The two craters are interpreted as products of the same eruptive system and share a common magmatic and depositional history

https://doi.org/10.5194/egusphere-2026-4195
Preprint. Discussion started: 17 August 2026

(Louie and Ruprecht, 2021; Morrison, 1964; Russell, 1885). This study focuses on the Big Soda Lake maar, an approximately 1.5 km^2 lake-filled crater that preserves the most extensive exposed stratigraphic record of the eruption.

The Soda Lake volcanic center forms part of a broader province of late Quaternary basaltic volcanism within the northern Walker Lane and western Basin and Range Province. Volcanism in this region has been linked to localized mantle melting associated with crustal extension and transtensional deformation (Bennett et al., 2003; Faulds et al., 2005). Although numerous small basaltic volcanic centers occur throughout western Nevada, robust eruption chronologies remain unavailable for many of these centers. Consequently, regional spatial and temporal patterns of Quaternary volcanism remain incompletely resolved, highlighting the importance of developing direct chronologic constraints for individual volcanic centers such as Soda Lake.

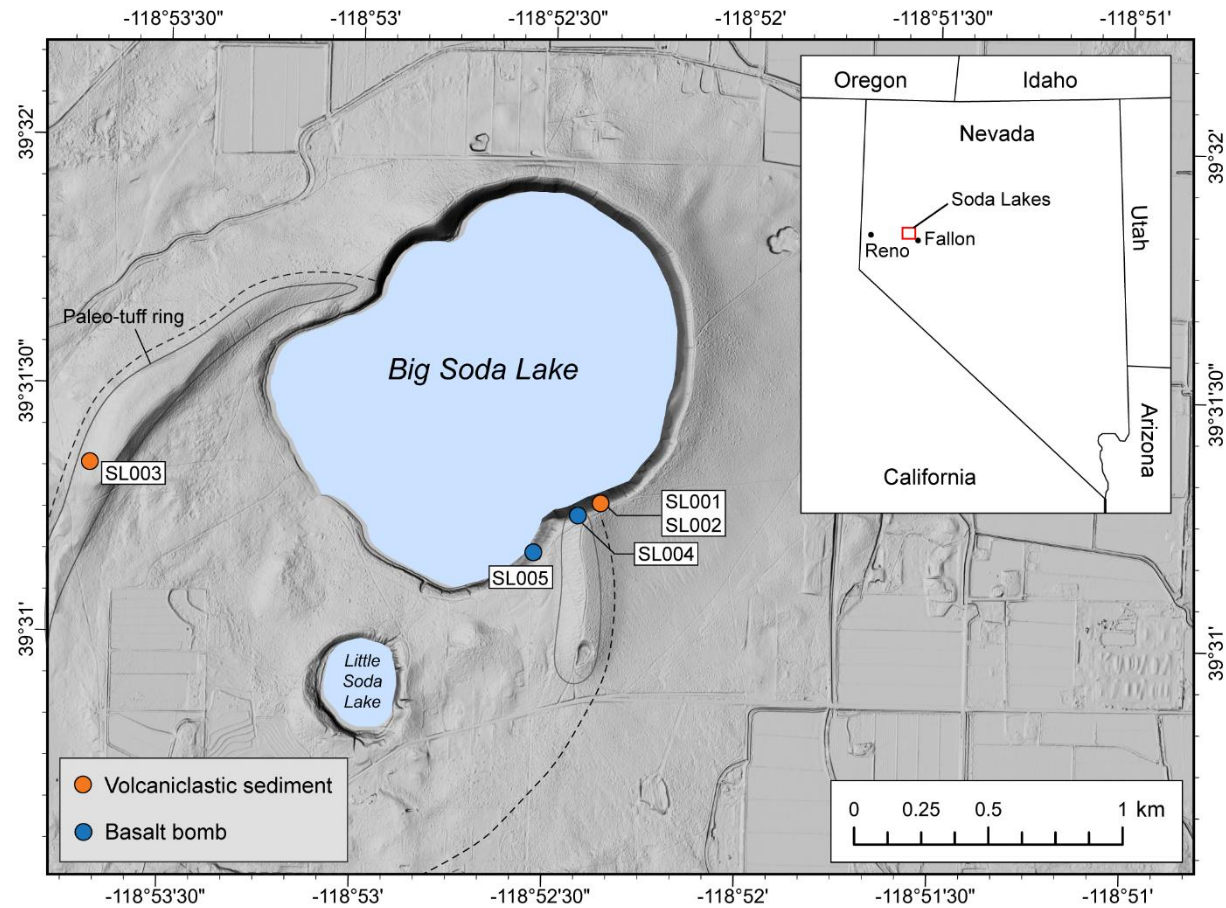

Figure 1. Hillshade map of the Soda Lake volcanic center in western Nevada showing sample locations and major geomorphic features. Orange symbols indicate volcaniclastic sediment samples and blue symbols indicate juvenile basalt bomb samples collected for luminescence dating. Samples SL001 and SL003 were collected from volcaniclastic deposits associated with the tuff cone, whereas samples SL004 and SL005 were obtained from *in-situ* basalt bombs partially buried within volcaniclastic

https://doi.org/10.5194/egusphere-2026-4195
Preprint. Discussion started: 17 August 2026

sediments along the south-eastern margin of Big Soda Lake. Sample SL003 was collected from reworked deposits exposed along the western paleo-tuff ring remnant. The dashed line represents the inferred extent of the ~12.5 ka crater margin. Base imagery consists of hillshade relief generated from a USGS 3DEP digital elevation model (U.S. Geological Survey, 2024).

The Big Soda Lake tuff cone has previously been subdivided into three principal stratigraphic units separated by unconformities that record multiple eruptions during the late Quaternary (Morrison, 1964; Russell, 1885). Much of the lower stratigraphy has been submerged following an ~18 m rise in lake level associated with construction of the Newlands Irrigation Project, leaving only the uppermost unit exposed above modern lake level. Consequently, the stratigraphic framework summarized here relies primarily on earlier descriptions, supplemented by limited modern observations.

The lower and middle units, now largely submerged, consist of bedded basaltic lapilli interbedded with lacustrine sediments and record early eruptive activity interspersed with periods of Lake Lahontan deposition. The upper unit forms the exposed tuff cone and reaches a maximum thickness of ~37 m. It is composed of interbedded lapilli-rich sands, pebbly sands, and minor gravel, locally containing basalt bombs with abundant calcic plagioclase and olivine phenocrysts. Frequent xenoliths up to 10 cm in diameter are also present. The tuff cone is capped by poorly sorted deposits interpreted as subaerial in origin (Figure 2). Although internal subdivisions of the upper unit have been described previously, only the uppermost portions are currently accessible along steep, unconsolidated crater walls. Importantly, the tuff cone is constructed on Lake Lahontan deposits, providing a clear stratigraphic constraint that eruptive activity post-dated deposition associated with the late Pleistocene Lake Lahontan highstand at ~11.5 ka (Adams et al., 2008).

Evidence for an earlier eruption is preserved southeast and southwest of Big Soda Lake, where a low (~17 m-high) ridge interpreted as a paleo-tuff ring is partially buried by lacustrine and aeolian sediments (Figure 1). The ridge exhibits multiple wave-cut shorelines and surface tufa deposits, indicating submergence during latest Pleistocene Lake Lahontan highstands, and is overlain to the north by younger shoreline-free tephra deposits. A soil pit excavated on the ridge exposed ~20 cm of laminated Lake Lahontan sands and tufa overlying medium sands and pebbles containing basaltic lapilli and ash, indicating incorporation of reworked pre-Holocene pyroclastic material. Additional support for older eruptions comes from well logs analyzed by Morrison (1964), which document cinder-rich deposits beneath lacustrine silts and clays and an upper volcanic ash unit attributed to the youngest eruption.

Together, the geomorphic preservation, stratigraphic framework, and evidence for multiple eruptions make the Soda Lake volcanic center well suited for direct geochronologic investigation.

3 Previous age constraints for the Soda Lakes eruption

The timing of eruptive activity at Soda Lakes remains poorly constrained. Stratigraphic relationships indicate that the most recent eruption post-dates the Lake Lahontan highstand at ~11.5 ka (Adams et al., 2008). Additional age constraints come from a single sediment core collected from the center of Big Soda Lake (Rosen et al., 2021). A radiocarbon age obtained from

https://doi.org/10.5194/egusphere-2026-4195
Preprint. Discussion started: 17 August 2026

fossil pollen concentrates at the base of the core (8.4 m depth) suggests that lake formation may have begun in the latest Pleistocene (~14.7 ka). However, radiocarbon ages throughout much of the overlying section (approximately 3-8 m depth) cluster between ~4 and 6 ka but are not stratigraphically coherent and do not follow superpositional order. Rosen et al. (2021) interpret these age reversals as the result of sediment disturbance, including slumping and mass movement, possibly related to interaction with the maar diatreme, rather than continuous sediment accumulation. Attempts to apply $^{40}Ar/^{39}Ar$ dating to the volcanic products at the Soda Lake volcanic center have been unsuccessful because of insufficient radiogenic Ar accumulation (J. Price, pers. comm., 2022). These limitations motivate the application of luminescence dating to volcanic and volcaniclastic materials directly associated with the Soda Lake eruptive sequence.

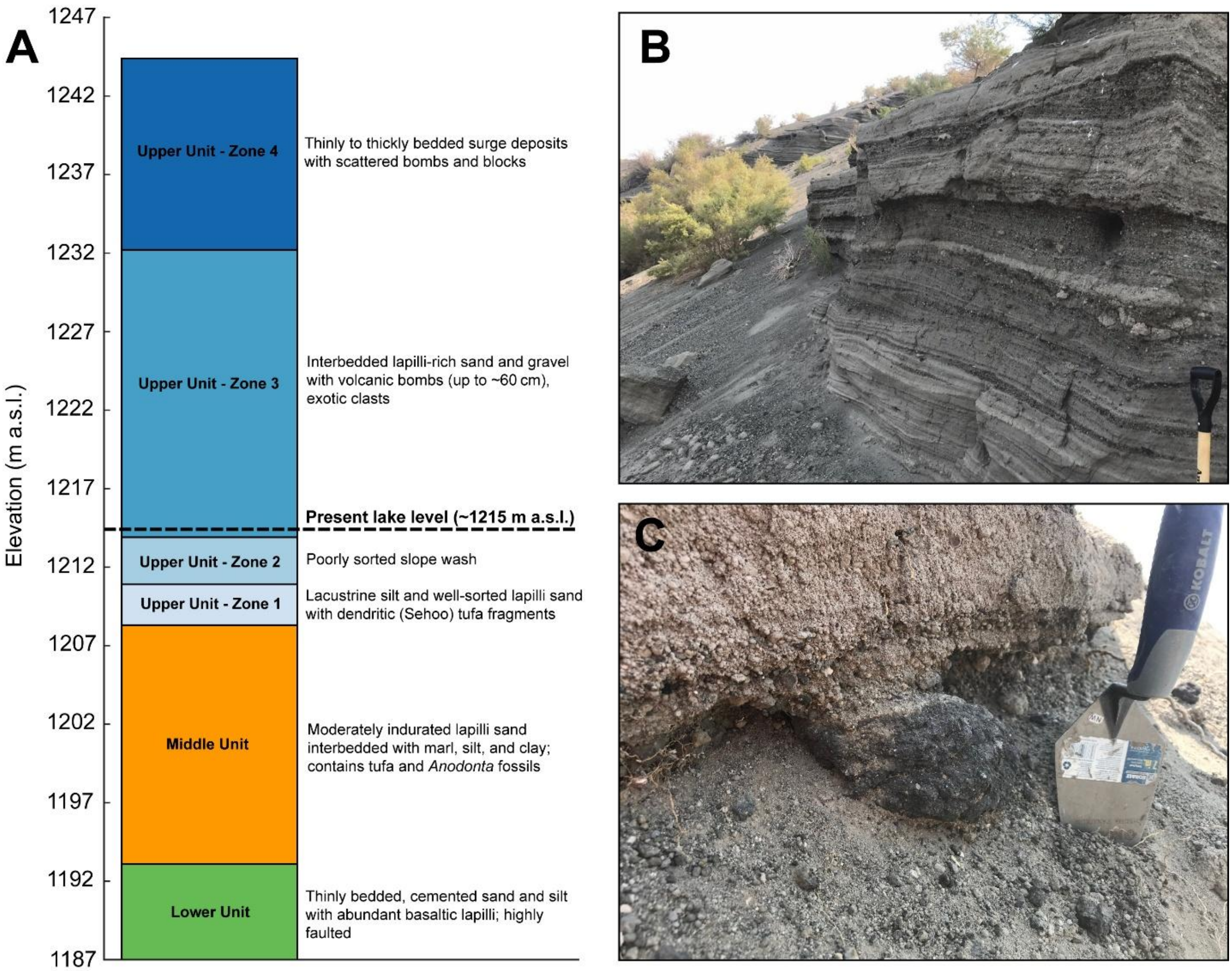

Figure 2. Stratigraphy and representative field photographs of volcaniclastic deposits exposed along the Big Soda Lake tuff cone. (A) Generalized stratigraphic column showing major lithostratigraphic units and interpreted depositional facies exposed above the modern lake level (~1215 m a.s.l.), adapted from Morrison (1964) and Russell (1885). The section

https://doi.org/10.5194/egusphere-2026-4195
Preprint. Discussion started: 17 August 2026

consists of interbedded phreatomagmatic surge deposits, lapilli-rich sands and gravels, lacustrine sediments, and bomb-bearing horizons. (B) Thinly to thickly bedded surge deposits within the upper part of the section at ~ 6 m depth displaying well-developed planar bedding and cross stratification characteristic of phreatomagmatic deposition (~7 m depth). (C) Juvenile basalt bomb partially buried within volcaniclastic sediments from the upper unit.

4 Methods

4.1 Sample collection and preparation

Four samples were collected from the Soda Lake volcanic center to target eruptive products representative of the most recent volcanic activity and, where possible, older eruptions.

Samples SL001 and SL002 were collected from the uppermost exposed portion of the Big Soda Lake tuff cone using stainless-steel tubes ~2 inches in diameter and ~6 inches in length. Sampling targeted laminated surge deposits interpreted as primary phreatomagmatic ejecta (Figure 2B). Care was taken to target *in-situ*, minimally disturbed material and to avoid areas affected by slope wash, bioturbation, or anthropogenic disturbance. Sample SL003 was collected from the paleo-tuff ring ridge located south of the main Big Soda Lake edifice using a hand auger. This sample targeted deposits that are interpreted to be from an older eruption.

Samples SL004 and SL005 consist of large juvenile basalt bombs, approximately 20 cm in diameter, collected *in-situ* from volcaniclastic deposits exposed in the upper part of the tuff cone (Figure 2C). The bombs were partially buried within surrounding volcaniclastic material and showed no evidence of post-depositional transport. These samples were targeted for extraction of plagioclase phenocrysts for luminescence analysis. The largest available bombs were preferentially selected to minimize complications associated with external gamma dose rate calculations and to reduce the relative gamma influence of surrounding sediments.

Preparation and luminescence analysis of the samples was conducted at the Desert Research Institute (DRI) Luminescence Research Laboratory in Reno, Nevada.

For sediment samples SL001, SL002, and SL003, approximately 3 cm of material from both ends of each sampling tube was removed and reserved for moisture content determination and dose rate measurements. The remaining interior material was prepared for luminescence analysis by first treating samples with sodium pyrophosphate decahydrate ($Na_4P_2O_7 \cdot 10H_2O$) to deflocculate clays, followed by wet sieving to isolate the 180-220 µm grain-size fraction. Carbonates and organic matter were removed using successive treatments with 10% HCl and 30% H_2O_2, respectively. Magnetic minerals were separated using a hand magnet, after which density separation with lithium heteropolytungstate was used to isolate the <2.58 g/cm^3. Density separation targeting the <2.58 g/cm^3 fraction was intended to concentrate potassium-rich feldspar grains, although the resulting separates may include minor contributions from other low-density feldspar phases. The resulting potassium-rich separates were etched in 10% hydrofluoric acid for 10 minutes to remove the outer alpha-irradiated rind and subsequently treated overnight in 10% HCl to dissolve fluoride precipitates.

https://doi.org/10.5194/egusphere-2026-4195
Preprint. Discussion started: 17 August 2026

For basalt bomb samples SL004 and SL005, preparation targeted the centermost portion of each bomb to minimize the effects of external dose-rate heterogeneity. Each bomb was cored through its center using a 1 cm diameter diamond coring drill (Hilti DD 120) operated under wet conditions, and an approximately 5 cm-long section corresponding to the core interior was isolated using a low-speed precision saw (Buehler IsoMet). The extracted material was gently crushed to disaggregate the grains using a mortar and pestle and wet-sieved to isolate the 90-220 µm grain-size fraction. Plagioclase was then separated using lithium heteropolytungstate to isolate the 2.70-2.76 g/cm^3 fraction and etched following the same hydrofluoric acid and HCl procedures described for the sediment samples. The resulting plagioclase separates were used for luminescence analysis.

4.2 Luminescence measurements and analysis

Luminescence measurements were performed using an automated Risø TL/OSL DA-20 luminescence reader housed at the DRI Luminescence Research Laboratory. Single-grain measurements were conducted on sediment samples SL001, SL002, and SL003 using a focused infrared laser (830 nm) delivering ~150 mW cm^2 at the sample position, enabling evaluation of grain-scale dose variability and incomplete bleaching. Feldspar separates from juvenile basalt bombs (samples SL004 and SL005) were measured using small multigrain aliquots (~2 mm diameter, ~30 grains per aliquot) stimulated by a cluster of infrared diodes with a peak emission at 870 nm and a maximum power of ~145 mW cm^2. Luminescence emissions were detected through a Corning/Kopp 7-59 and Schott BG39 filter combination (transmitting ~320-460 nm) using a H7360-02 UV/VIS photomultiplier tube.

For samples SL001, SL002, and SL003, equivalent doses (D_e) were determined using a post-IRIR$_{150}$ single-aliquot regenerative-dose (SAR) protocol (Murray and Wintle, 2000, 2003; Reimann and Tsukamoto, 2012; Wallinga et al., 2000). This approach involves sequential stimulation of feldspar, first using a low-temperature infrared signal at 50 °C (IR$_{50}$), followed by a post-IRIR signal measured at 150 °C (post-IRIR$_{150}$). While IR$_{50}$ signals are generally more sensitive to resetting under light exposure, they are prone to significant anomalous fading. In contrast, low temperature pIRIR signals exhibit improved signal stability while retaining relatively efficient bleaching behavior, commonly resulting in small residual doses (<0.2 Gy) for well-reset grains (Reimann and Tsukamoto, 2012). In view of the likelihood of incomplete bleaching in the sampled deposits and the low D_e values observed during initial testing, the pIRIR$_{150}$ signal was adopted for D_e determination. Performance of the pIRIR$_{150}$ protocol was evaluated using dose-recovery tests and residual dose measurements after 24 h of bleaching using a SOL2 solar simulator.

For basalt bomb samples SL004 and SL005, D_e values were determined using the post-IR IRSL signal measured at 225 °C (post-IRIR$_{225}$; Buylaert et al., 2009). This signal was selected to maximize signal stability and minimize anomalous fading, and because plagioclase phenocrysts extracted from bomb interiors are expected to have experienced complete thermal resetting during eruption.

Dose-response curves for individual grains and aliquots were fitted using single-saturating exponential functions. Standard rejection criteria were applied to screen unsuitable measurements, including: (i) poor signal intensity, defined as a net natural test-dose (T_n) signal less than three times the background standard deviation; (ii) recycling ratios deviating by more

https://doi.org/10.5194/egusphere-2026-4195
Preprint. Discussion started: 17 August 2026

than 20% from unity; (iii) test-dose uncertainties exceeding 20%; and (iv) excessive recuperation, defined as L_x/T_x values following the zero-dose regenerative step exceeding 5% of the sensitivity-corrected natural signal (L_n/T_n).

D_e distributions were evaluated using overdispersion values and Abanico plots to assess scatter and guide statistical age-model selection. Samples SL001, SL002, and SL003 exhibited high overdispersion and positively skewed post-IRIR$_{150}$ D_e distributions, consistent with incomplete bleaching; burial doses for these samples were therefore estimated using the Minimum Age Model (MAM, Galbraith et al., 1999). In contrast, basalt bomb samples SL004 and SL005 displayed low overdispersion and relatively symmetric D_e distributions, indicating a more uniform dose population, and burial doses were calculated using the Central Age Model (CAM, Galbraith et al., 1999).

Fading rates (g-values) were measured for the post-IRIR$_{150}$ and post-IRIR$_{225}$ signals over the course of ~1 week on six discs of each sample using the approach of Auclair et al. (2003) after D_e measurements were completed. Final ages of these samples were corrected for fading using the weighted mean fading rates for each sample and the correction model of Huntley and Lamothe (2001).

4.3 Dosimetry

Total environmental dose rates were calculated as the sum of external beta, gamma, and cosmic radiation contributions, as well as internal contributions. For all samples, uranium, thorium, and potassium concentrations were determined from dried, milled subsamples analyzed at ALS Geochemistry. Uranium and thorium were measured by ICP-MS following lithium borate fusion, while K_2O was measured by ICP-AES and converted to percent potassium. Dose rates (Gy/ka) were calculated using the conversion factors of Liritzis et al. (2013). Beta dose rates were corrected using grain-size attenuation factors following Guérin et al. (2011) and etch-depth attenuation factors of (Brennan 2003).

For sediment samples (SL001, SL002, and SL003), external gamma dose rates were measured *in-situ* using a portable NaI Canberra Inspector 1000 gamma spectrometer. Internal dose rates were calculated assuming a potassium concentration of 12.5 ± 0.5% for K-feldspar (Huntley and Baril, 1997).

For basalt bomb samples (SL004 and SL005), both the external gamma contribution from surrounding sediments and the self-dose contribution from the bomb material were considered. Gamma dose rate contributions from the bomb interior and surrounding sediments were calculated as a function of distance from the luminescence sample and respective material densities, accounting for geometric attenuation (Aitken, 1985). Internal dose rates for bomb samples were calculated assuming a potassium concentration of 0.2 ± 0.1% for calcic plagioclase (DGIS Team, 2024), with average crystal sizes estimated from microscopic inspection.

All dose rates were corrected for long-term moisture content assuming a water content of 0 ± 0% for the juvenile basalt bomb samples and 1 ± 5% for the volcaniclastic sediment samples. Cosmic dose rate contributions were calculated based on sample depth, elevation, and geographic position (Prescott and Hutton, 1994).

https://doi.org/10.5194/egusphere-2026-4195
Preprint. Discussion started: 17 August 2026

5 Results

5.1 Luminescence signal behaviour and D_e distributions

Samples SL001, SL002, and SL003 produced sufficiently bright post-$IRIR_{150}$ signals suitable for D_e determination (Figure 3). Dose-recovery tests conducted on the post-$IRIR_{150}$ signal reproduced the administered laboratory dose within 10%, confirming the suitability of the applied SAR protocol for these samples. Residual doses measured after 24 h of solar-simulator exposure were low (0.3-0.6 Gy for post-$IRIR_{150}$) and were not applied as corrections in the age calculations. Anomalous fading rates (g-values) measured for the same signal ranged from 1.8 to 2.1 %/decade. The post-$IRIR_{150}$ signals exhibited broad, positively skewed equivalent dose distributions for these samples with overdispersion values >60% (Figure 3), consistent with heterogeneous resetting before burial.

In contrast, plagioclase phenocrysts extracted from basalt bombs SL004 and SL005, measured using post-$IRIR_{225}$ on small multigrain aliquots, produced narrow, near-Gaussian D_e distributions with low overdispersion (Figure 3), consistent with complete thermal resetting during eruption. Average anomalous fading rates for SL004 and SL005 were 1.2 ± 0.13 %/decade and 1.4 ± 0.17 %/decade, respectively.

https://doi.org/10.5194/egusphere-2026-4195
Preprint. Discussion started: 17 August 2026

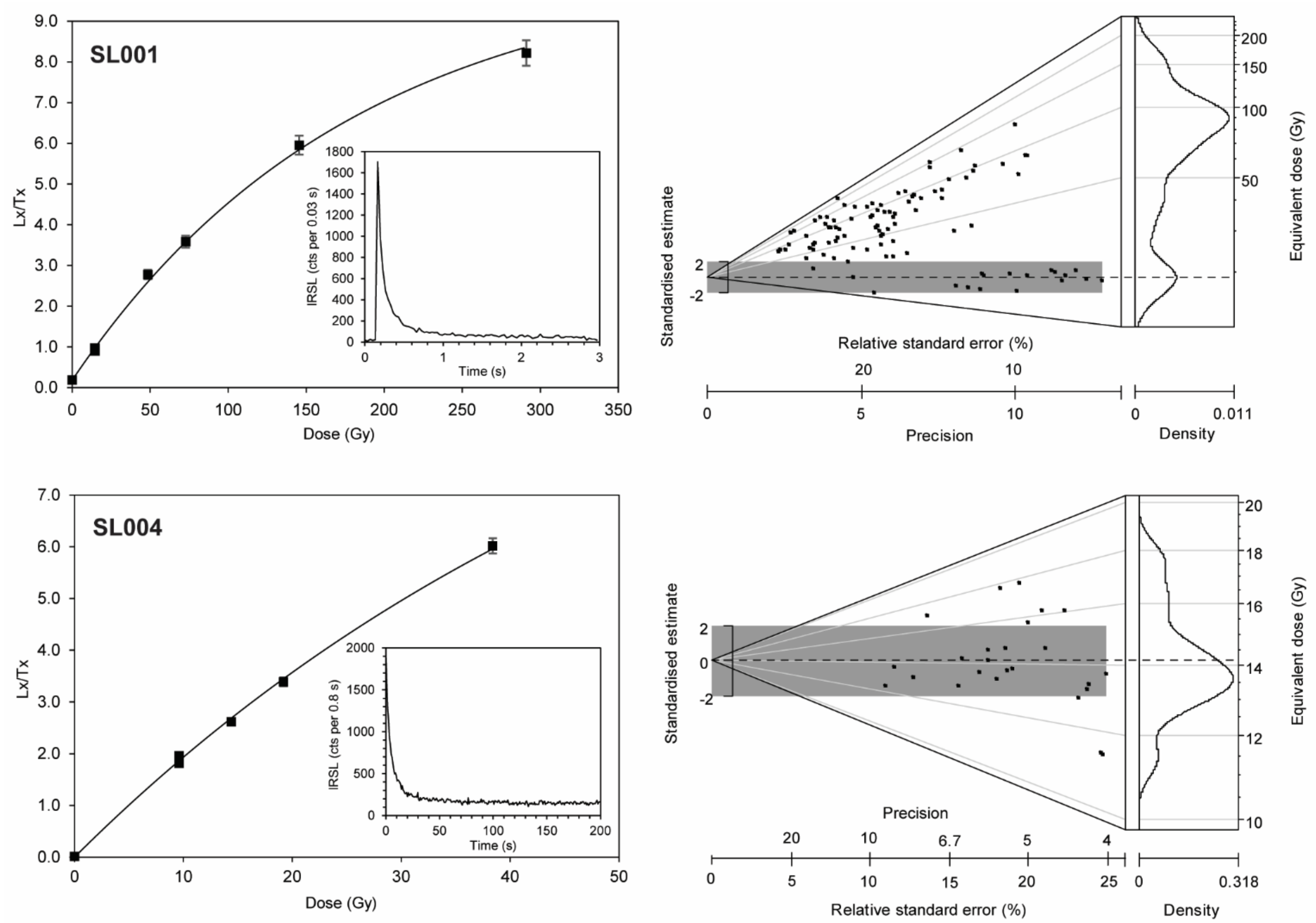

Figure 3. Representative luminescence characteristics and equivalent dose (D_e) distributions for volcaniclastic sediment sample SL001 and juvenile basalt bomb sample SL004. Left panels show representative post-IRIR dose-response curves together with the corresponding natural luminescence decay curves (insets). Right panels show Abanico plots of the equivalent dose distributions. Dashed horizontal lines represent the D_e estimates calculated using the Minimum Age Model (SL001) and Central Age Model (SL004), respectively. Shaded bands indicate the ±2σ uncertainty envelope surrounding each D_e estimate, and kernel density functions are shown along the right side of each Abanico plot. Additional Abanico plots for all measured samples and luminescence signals are provided in Figure S1.

5.2 Luminescence ages

Equivalent dose estimates derived from post-IRIR$_{150}$ single-grain measurements (SL001, SL002, SL003) and post-IRIR$_{225}$ multigrain measurements (SL004, SL005) were combined with total dose rates to calculate luminescence ages (Table 1). Total dose rates range from 2.47 to 4.28 Gy/ka and reflect differences in sample geometry, internal potassium content, and

https://doi.org/10.5194/egusphere-2026-4195
Preprint. Discussion started: 17 August 2026

external gamma contributions between sediment and bomb samples. A complete breakdown of the individual dose rate components is provided in Table S1.

Sediment samples SL001 and SL002, collected from surge deposits associated with the youngest exposed eruption of the Soda Lake volcanic center, yielded luminescence ages of 5.46 ± 0.53 ka and 5.19 ± 0.53 ka (error is 1 sigma), respectively. In contrast, sample SL003, collected from reworked volcaniclastic deposits exposed within the paleo-tuff ring remnant west of Big Soda Lake, yielded an older luminescence age of 12.56 ± 0.99 ka. All sediment ages were calculated using Minimum Age Model D_e values. Basalt bomb samples SL004 and SL005 yield ages of 5.72 ± 0.46 ka and 5.46 ± 0.43 ka, respectively, calculated using Central Age Model D_e values. Ages derived from sediment and bomb samples associated with the youngest eruption overlap within uncertainty, indicating internal consistency among independent materials and measurement approaches. All reported ages are presented at 1σ uncertainty and include contributions from D_e and total dose rate (Table 1).

Table 1. Summary of equivalent dose and luminescence age data.

Sample ID	Sample type	Lat/long coordinates	Depth (m)	N[a]	OD (%)	D_e (Gy)[b]	No. of saturated grains	g-value (%/decade)	Total dose rate (Gy/ka)	Uncorrected MAM Age (ka)[c]	Fading-corrected MAM Age (ka)[c]
SL001	Sediment	39.521029°, 118.873381°	6.00	100 (1000)	66 ± 5	18.86 ± 1.47	46	1.80 ± 0.15	4.01 ± 0.26	4.71 ± 0.48	5.46 ± 0.53
SL002	Sediment	39.521029°, 118.873381°	5.85	92 (1000)	63 ± 5	18.88 ± 1.62	51	1.99 ± 0.18	4.28 ± 0.28	4.41 ± 0.47	5.19 ± 0.53
SL003	Sediment	39.523075°, 118.894269°	0.75	131 (1000)	55 ± 4	39.24 ± 2.05	43	2.12 ± 0.19	3.75 ± 0.25	10.46 ± 0.85	12.56 ± 0.99
SL004	Bomb	39.520835°, 118.874145°	5.00	25 (30)	0 ± 0	14.14 ± 0.45	0	1.40 ± 0.14	2.76 ± 0.17	5.13 ± 0.36	5.72 ± 0.46
SL005	Bomb	39.519884°, 118.875632°	4.10	17 (30)	0 ± 0	12.40 ± 0.51	0	1.10 ± 0.13	2.47 ± 0.17	5.01 ± 0.40	5.46 ± 0.43

[a] N is the number of equivalent dose, D_e, determinations accepted after screening. In parentheses are the total number of grains or aliquots measured.

[b] For sediment samples, the D_e was determined using the Minimum Age Model (MAM, Galbraith et al., 1999); for bombs samples, the D_e was determined using the Central Age Model (MAM, Galbraith et al., 1999). The D_e values incorporate a σ_b of 0.15. The reported error is the standard error.

[c] Luminescence ages, rounded to the nearest 10 years, are expressed as thousands of years before AD 2024. Error is 1 sigma.

https://doi.org/10.5194/egusphere-2026-4195
Preprint. Discussion started: 17 August 2026

6 Discussion

6.1 Eruption age of the Soda Lake volcanic center

Luminescence ages derived from volcaniclastic sediments and juvenile basalt bombs provide the first direct chronologic constraints on the Soda Lake volcanic center based on materials intrinsic to the eruption itself. Ages obtained from laminated surge deposits and bombs within the exposed Big Soda Lake tuff cone (SL001, SL002, SL004, SL005) cluster at ~5.5 ka despite being derived from different materials, luminescence signals, and statistical age models. This younger eruption coincides with the prominent cluster of radiocarbon ages between ~5.7 and 5.3 cal ka reported from the Big Soda Lake sediment core by Rosen et al. (2021). Rosen et al. (2021) noted that these ages were stratigraphically inconsistent and suggested they may reflect large-scale sediment disturbance and slumping within the lake basin rather than primary depositional ages. However, our results indicate that these radiocarbon ages may nevertheless provide a valid constraint on the timing of the most recent eruption.

In contrast, sample SL003, collected from the paleo-tuff ring remnant west of the Big Soda Lake maar, yielded a significantly older post-IRIR$_{150}$ age of ~12.5 ka, broadly consistent with the basal ~14.7 cal ka age identified at the base of the Big Soda Lake core sequence (Rosen et al., 2021). Although minor post-depositional reworking cannot be excluded, the stratigraphic position of the deposit and its association with the paleo-tuff ring strongly suggest that this age closely approximates the timing of an older eruption. The correspondence between the ~5.5 ka luminescence ages and the younger radiocarbon cluster suggests that at least some of the mid-Holocene ages identified by Rosen et al. (2021) may instead reflect a distinct eruption preserved within the basin stratigraphy. Conversely, the older basal ~14.7 cal ka age identified by Rosen et al. (2021) may record an earlier eruption, an interpretation further supported here by geomorphic evidence for a distinct paleo-tuff ring west and southwest of Big Soda Lake. Together, these results support the interpretation of at least two late Quaternary volcanic eruptions at the Soda Lake volcanic center.

The agreement between ages derived from volcaniclastic sediments and juvenile basalt bombs is particularly significant given the contrasting luminescence characteristics and dose-rate environments of the dated materials. Potassium-rich feldspar derived from volcaniclastic sediments yielded broad and positively skewed D_e distributions consistent with heterogeneous resetting, whereas plagioclase phenocrysts extracted from juvenile basalt bombs produced narrow and symmetrical dose distributions indicative of more uniform resetting histories. Despite these differences, ages overlap within uncertainty, suggesting that the applied statistical approaches and dose-rate models effectively capture the timing of eruption.

The luminescence chronology also provides new insight into the relationship between eruptive activity and late Quaternary hydrologic evolution of the Lahontan Basin (Figure 4). The older eruption at ~12.5 ka occurred during the final stages of regression from the Lake Lahontan highstand, when lake levels remained sufficiently elevated to inundate portions of the paleo-tuff ring now preserved south and southwest of Soda Lake. Wave-cut shorelines and tufa deposits developed on the paleo-tuff ring indicate that these deposits predate final desiccation of the basin and were submerged during the latest Pleistocene lake highstand. In contrast, the younger eruption at ~5.5 ka post-dates Pleistocene Lake Lahontan.

https://doi.org/10.5194/egusphere-2026-4195
Preprint. Discussion started: 17 August 2026

These relationships suggest that phreatomagmatic activity at the Soda Lake volcanic center was not restricted to periods of maximum lake extent but instead persisted across major hydrologic transitions within the Lahontan Basin. The younger eruption demonstrates that shallow groundwater systems capable of sustaining explosive magma-water interaction remained present long after recession of pluvial Lake Lahontan. This interpretation is consistent with the internally drained hydrogeologic setting of the Carson Sink region, where shallow groundwater and localized basin-floor saturation likely persisted despite large-scale regression of surface water bodies (Adams et al., 2008). These conditions for potential future magma-groundwater interaction continue into today with the water table high enough to sustain lakes in Big and Little Soda Lake craters.

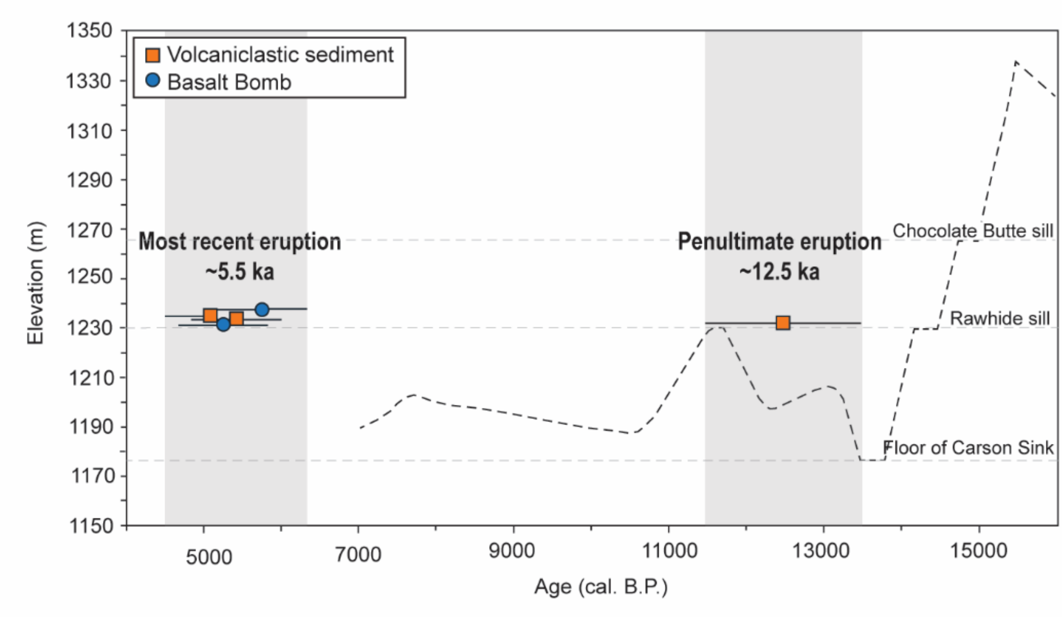

Figure 4. Luminescence age constraints for late Quaternary eruptive activity at the Soda Lake volcanic center relative to reconstructed lake-level fluctuations in the Lahontan Basin, adapted from Adams et al. (Adams et al., 2008). The dashed curve represents generalized late Quaternary lake-level fluctuations in the Carson Sink region based on previous paleohydrologic reconstructions (Adams et al., 2008). Orange squares represent ages derived from volcaniclastic sediments and blue circles represent ages obtained from plagioclase phenocrysts extracted from juvenile basalt bombs. Horizontal bars indicate ±1σ age uncertainties. Results identify two late Quaternary eruptions at approximately 12.5 ka and 5.5 ka. The younger eruptive phase post-dates regression of Lake Lahontan and corresponds to deposits exposed within the modern Soda Lake tuff cone, whereas the older eruptive phase is associated with the paleo-tuff ring remnant partially submerged during latest Pleistocene lake highstands.

https://doi.org/10.5194/egusphere-2026-4195
Preprint. Discussion started: 17 August 2026

6.2 Luminescence resetting pathways in volcaniclastic systems

Luminescence resetting in volcanic environments is commonly attributed to optical bleaching during transport and deposition and/or thermal resetting associated with eruptive heating (Fattahi and Stokes, 2003). However, in volcaniclastic settings, resetting pathways may be substantially more complex because grains can experience highly variable combinations of transient heating, sunlight exposure, fragmentation, and mechanical stress during eruption (Dufek, 2016). The contrasting D_e distributions observed between volcaniclastic sediments and juvenile basalt bombs at Soda Lake likely reflect differing combinations of resetting processes and depositional histories (Figure 5).

Plagioclase phenocrysts hosted within juvenile basalt bombs were very likely fully thermally reset during eruption and emplacement. The symmetric D_e distributions and comparatively low overdispersion values observed in these samples are consistent with relatively homogeneous resetting and support the application of multigrain measurements and Central Age Models for age determination. Because plagioclase phenocrysts within basalt bombs were reset thermally rather than optically, eruption ages derived from these materials are comparatively insensitive to incomplete bleaching effects that commonly complicate volcaniclastic deposits. In contrast, volcaniclastic sediments from the tuff ring deposits likely experienced more heterogeneous resetting histories. These deposits contain mixtures of juvenile volcanic material and entrained basin-floor sediment that may have retained variable inherited luminescence signals prior to eruption. Consequently, single-grain measurements and Minimum Age Models were required to isolate the youngest and ostensibly most completely reset grain populations.

While optical and thermal resetting pathways in volcanic systems are comparatively well understood, the potential role of mechanical stress as a luminescence resetting mechanism remains poorly constrained, particularly in volcaniclastic environments. Experimental and field-based studies have demonstrated that luminescence signals may be modified through frictional heating, grain-to-grain stress, comminution, and mechanical deformation in subglacial sediments and fault gouges (Bateman et al., 2018; Swift et al., 2011; Toyoda et al., 2000; Yang et al., 2019; Zöller et al., 2009). Ring-shear experiments conducted by Bateman et al. (2018) demonstrated that localized grain stresses generated during sediment shearing can produce partially or fully reset grains even in the absence of light exposure. Similar processes may plausibly occur during phreatomagmatic eruptions, where highly energetic fragmentation, particle collisions, and abrasive transport may contribute to luminescence signal resetting during eruption and emplacement. Although the present dataset cannot independently isolate the contribution of mechanically induced resetting, the contrasting D_e distributions observed between volcaniclastic sediments and thermally reset bomb phenocrysts suggest that multiple resetting pathways likely operated during eruption. Importantly, if mechanically mediated partial resetting occurs within tephra clouds, the resulting luminescence characteristics may retain information related to eruption conditions, including tephra density, temperature, fragmentation intensity, and internal particle dynamics. If confirmed through future experimental studies, such a relationship would open an entirely new avenue for using luminescence signals to investigate syn-eruptive processes during explosive volcanic events.

https://doi.org/10.5194/egusphere-2026-4195
Preprint. Discussion started: 17 August 2026

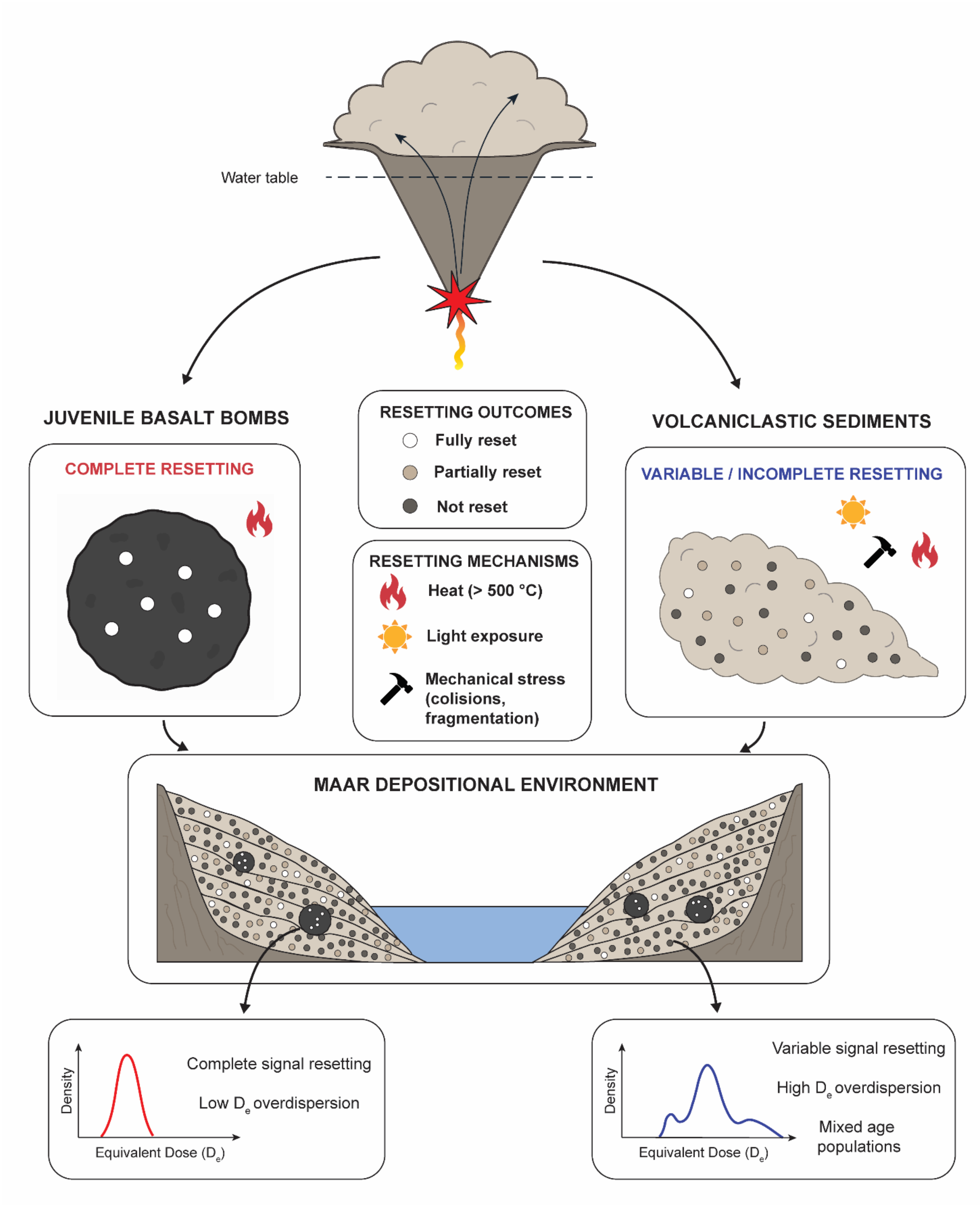

https://doi.org/10.5194/egusphere-2026-4195
Preprint. Discussion started: 17 August 2026

Figure 5. Conceptual model illustrating contrasting luminescence resetting pathways in maar volcanic systems. Juvenile basaltic bombs are derived directly from magma and experience prolonged high-temperature exposure during eruption and transport, resulting in complete thermal resetting and a homogeneous population of fully reset grains. In contrast, surge-transported volcaniclastic material comprises a mixture of juvenile volcanic particles, fragmented country rock, and liberated mineral crystals that experience variable combinations of thermal, optical, and mechanical resetting during transport within pyroclastic surges. These processes generate heterogeneous grain populations containing fully reset, partially reset, and inherited luminescence signals. Following deposition within crater-wall deposits, these contrasting resetting histories are reflected in the resulting equivalent dose (D_e) distributions, with thermally reset juvenile bombs expected to yield low overdispersion populations, whereas mixed volcaniclastic deposits may exhibit elevated overdispersion and complex D_e distributions resulting from incomplete resetting.

6.3 Comparison with previous luminescence applications to volcanic materials

The application of luminescence dating to volcanic deposits has evolved considerably over the past several decades as understanding of eruption-related signal resetting and luminescence behavior has improved. As summarized by (Bösken and Schmidt, (2020), direct luminescence dating has been applied to three principal components of tephra: (1) volcanic glass shards, (2) juvenile volcanic quartz and feldspar contained within eruptive products, and (3) quartz or feldspar fragments derived from shattered country rock. These materials record different eruption-related resetting mechanisms and therefore present distinct challenges related to signal stability and the completeness of resetting.

Early studies focused primarily on volcanic glass and juvenile volcanic minerals, demonstrating the potential for directly dating volcanic eruptions while also highlighting challenges associated with anomalous fading, signal instability, and incomplete resetting (e.g., (Berger, 1991; Berger and Huntley, 1994; Tsukamoto et al., 2007; Wintle, 1973). Subsequent methodological advances, including red thermoluminescence and elevated-temperature luminescence signals, substantially improved the potential for dating juvenile volcanic minerals (e.g., Biswas et al., 2013; Rodrigues et al., 2022; Toyoda et al., 2006).

Direct luminescence dating has subsequently been extended to materials whose signals were reset during eruption rather than during crystallization. Early work demonstrated the feasibility of dating sediments baked beneath lava flows and rocks heated during lava emplacement (e.g., (Bassinet et al., 2006; Miallier et al., 1991; Pilleyre et al., 1992). More recently, workers have demonstrated that fragmented and thermally reset country rock in phreatomagmatic systems can also provide reliable eruption chronologies, emphasizing the importance of understanding the resetting history of the dated material and, where possible, comparing multiple luminescence signals (Preusser et al., 2011; Rufer et al., 2012; Schmidt et al., 2017a).

The Soda Lake study builds upon these previous applications by integrating two independent eruption-related archives within the same volcanic sequence: potassium-rich feldspar grains isolated from volcaniclastic deposits and plagioclase phenocrysts hosted within juvenile basalt bombs. Whereas previous studies have generally focused on a single material or resetting mechanism, the agreement between these independent archives demonstrates that reliable eruption chronologies can

https://doi.org/10.5194/egusphere-2026-4195
Preprint. Discussion started: 17 August 2026

be obtained from contrasting volcanic materials within the same eruptive system. This expands the range of materials that can be used for direct luminescence dating of volcanic eruptions and highlights the flexibility of the technique for young mafic volcanic systems.

Collectively, previous studies and the Soda Lake results demonstrate that no single material or approach is universally applicable to volcanic deposits. Instead, successful direct luminescence dating depends on selecting materials appropriate for the eruptive setting and evaluating their luminescence characteristics accordingly. Together with previous applications to volcanic glass, juvenile volcanic minerals, and thermally reset country rock, the present study further broadens the range of eruption-related materials that can be used to directly constrain eruption chronologies.

6.4 Implications for volcanism in the Lahontan Basin

The luminescence chronology presented here demonstrates that phreatomagmatic volcanism persisted within the Lahontan Basin into the late Quaternary during a period of major hydrologic transition following regression of Lake Lahontan. The results support previous interpretations that magma-groundwater interaction played a fundamental role in controlling eruptive style at the Soda Lake volcanic center and indicate that shallow groundwater systems remained capable of driving explosive basaltic volcanism in western Nevada.

The spatial association between nearby late Quaternary eruptive centers, including the Upsal Hogback volcanic center approximately 11 km north-northeast of Soda Lake, Quaternary faulting, and geothermal activity within the Soda Lake region (McLachlan, 2018; Olmsted et al., 1984) suggests that deformation associated with the northern Walker Lane likely enhanced crustal permeability and influenced magma ascent and vent localization within the Lahontan Basin. Although the eruptive history of the Upsal Hogback volcanic center remains only loosely constrained, geomorphic relationships with Lake Lahontan deposits suggest hydrovolcanic activity during the late Pleistocene (Adams et al., 2008). The north-northeast alignment of the Upsal Hogback vents, together with mapped faults and geothermal activity between the two volcanic centers, is consistent with regional structural control on vent localization, although the limited geochronologic constraints available for most late Quaternary volcanic centers in western Nevada currently preclude robust evaluation of regional eruptive patterns. Moreover, magmatism in the northern Walker Lane is more likely related to localized mantle upwelling and small-scale convective processes, as larger mantle-scale features proposed to drive decompression melting farther south, such as the Isabella Anomaly, are spatially removed from the Soda Lake region (Gazel et al., 2012).

The recognition of multiple eruptions at Soda Lakes also highlights the importance of developing robust chronologic frameworks for small basaltic volcanic fields in the western Great Basin. The presence of late Quaternary phreatomagmatic eruptions at Soda Lakes demonstrates that volcanism in the region is an active hazard that should be considered. Improved eruption chronologies therefore provide an important basis for evaluating the recurrence and distribution of volcanism in tectonically active intraplate settings.

https://doi.org/10.5194/egusphere-2026-4195
Preprint. Discussion started: 17 August 2026

7 Conclusions

This study provides the first direct luminescence-based age constraints for the Soda Lake volcanic center and represents the first published application of luminescence dating to Quaternary basaltic volcanism in the western United States. By targeting potassium-rich feldspar separates derived from volcaniclastic sediments and plagioclase phenocrysts extracted from juvenile basalt bombs, we establish a robust late Quaternary eruptive chronology based on materials intrinsic to the eruption itself.

Luminescence ages derived from single-grain post-$IRIR_{150}$ measurements of surge and reworked volcaniclastic deposits and post-$IRIR_{225}$ measurements of bomb-derived plagioclase converge on eruption ages despite contrasting resetting pathways and depositional histories. Bomb-derived plagioclase and potassium-rich volcaniclastic sediments record contrasting resetting histories yet yield internally consistent eruption ages. The resulting ages constrain the youngest exposed eruption at the Soda Lake eruptive center to approximately 5.5 ka, the youngest volcanic eruption in Nevada. Together with stratigraphic relationships associated with the paleo-tuff ring remnant, these data support interpretation of at least two late Quaternary eruptions at approximately 12.5 ka and 5.5 ka.

The refined chronology demonstrates that the youngest eruption post-dates the Lake Lahontan highstand and improves upon previous age interpretations based primarily on indirect stratigraphic relationships and radiocarbon dating of pollen in lacustrine sediments. These results highlight the limitations of relying solely on lacustrine stratigraphy to constrain eruption timing in internally drained basins and demonstrate the value of directly dating volcanic and volcaniclastic materials.

More broadly, this work demonstrates that luminescence dating provides a powerful and flexible framework for directly constraining the timing of young basaltic eruptions in settings where conventional radiometric techniques are ineffective because of low potassium contents and insufficient radiogenic argon accumulation. The agreement between eruption ages derived from potassium-rich volcaniclastic sediments and thermally reset plagioclase phenocrysts hosted within juvenile basalt bombs demonstrates that reliable eruption chronologies can be obtained from multiple independent eruptive materials characterized by fundamentally different resetting pathways. By demonstrating internally consistent eruption ages from volcaniclastic sediments and juvenile basalt bombs, this study builds upon previous applications of luminescence dating in volcanic settings and highlights the value of integrating multiple eruption-related materials to complement existing geochronologic approaches in young basaltic volcanic systems.

Data availability

Supplementary figures and tables supporting this study are provided in the Supplement. The raw equivalent dose (D_e) data underlying the luminescence age calculations are publicly available through Zenodo at https://doi.org/10.5281/zenodo.21746037

Author contributions

KR: Conceptualization, Methodology, Formal analysis, Investigation, Data curation, Writing – original draft, Writing – review & editing, Visualization, Project administration; PR: Conceptualization, Writing – review & editing; CD: Conceptualization, Writing – review & editing.

Competing interests

The authors declare that they have no conflict of interest.

Acknowledgements

K.R. thanks the Desert Research Institute (DRI) Micro Analysis and Visualization Laboratory for assistance with scanning electron microscopy and energy-dispersive X-ray spectroscopy analyses. K.R. also thanks Saige Howard for invaluable assistance with fieldwork as well as the DRI Luminescence Laboratory hourly staff for their assistance with sample preparation.

Financial support

This research was supported by internal funds provided to K.R. by the Desert Research Institute (DRI).

References

Adams, K. D., Goebel, T., Graf, K., Smith, G. M., Camp, A. J., Briggs, R. W., and Rhode, D.: Late Pleistocene and early Holocene lake-level fluctuations in the Lahontan Basin, Nevada: Implications for the distribution of archaeological sites, Geoarchaeology, 23, 608–643, 2008.

Aitken, M. J.: Thermoluminescence dating, Academic Press, London, 1985.

Auclair, M., Lamothe, M., and Huot, S.: Measurement of anomalous fading for feldspar IRSL using SAR, Radiat. Meas., 37, 487–492, 2003.

Bassinet, C., Mercier, N., Miallier, D., Pilleyre, T., Sanzelle, S., and Valladas, H.: Thermoluminescence of heated quartz grains: Intercomparisons between SAR and multiple-aliquot additive dose techniques, Radiat. Meas., 41, 803–808, 2006.

Bateman, M. D., Swift, D. A., Piotrowski, J. A., Rhodes, E. J., and Damsgaard, A.: Can glacial shearing of sediment reset the signal used for luminescence dating?, Geomorphology, 306, 90–101, 2018.

Bennett, R. A., Wernicke, B. P., Niemi, N. A., Friedrich, A. M., and Davis, J. L.: Contemporary strain rates in the northern Basin and Range province from GPS data, Tectonics, 22, 2003.

Berger, G. W.: The use of glass for dating volcanic ash by thermoluminescence, J. Geophys. Res. Solid Earth, 96, 19705–19720, 1991.

https://doi.org/10.5194/egusphere-2026-4195
Preprint. Discussion started: 17 August 2026

Berger, G. W. and Huntley, D. J.: Tests for optically stimulated luminescence from tephar glass, Quat. Sci. Rev., 13, 509–511, 1994.

Biswas, R. H., Williams, M. A. J., Raj, R., Juyal, N., and Singhvi, A. K.: Methodological studies on luminescence dating of volcanic ashes, Quat. Geochronol., 17, 14–25, 2013.

Bösken, J. J. and Schmidt, C.: Direct and indirect luminescence dating of tephra: A review, J. Quat. Sci., 35, 39–53, 2020.

Brennan, B. J.: Beta doses to spherical grains, Radiat. Meas., 37, 299–303, 2003.

Buylaert, J.-P., Murray, A. S., Thomsen, K. J., and Jain, M.: Testing the potential of an elevated temperature IRSL signal from K-feldspar, Radiat. Meas., 44, 560–565, 2009.

Dufek, J.: The fluid mechanics of pyroclastic density currents, Annu. Rev. Fluid Mech., 48, 459–485, 2016.

Fattahi, M. and Stokes, S.: Dating volcanic and related sediments by luminescence methods: a review, Earth. Sci. Rev., 62, 229–264, 2003.

Faulds, J. E., Henry, C. D., and Hinz, N. H.: Kinematics of the northern Walker Lane: An incipient transform fault along the Pacific–North American plate boundary, Geology, 33, 505–508, 2005.

Foeken, J. P. T., Stuart, F. M., and Francalanci, L.: Dating Holocene lavas on Stromboli, Italy using cosmogenic He, Quat. Geochronol., 4, 517–524, 2009.

Galbraith, R. F., Roberts, R. G., Laslett, G. M., Yoshida, H., and Olley, J. M.: Optical dating of single and multiple grains of quartz from Jinmium rock shelter, northern Australia: Part I, experimental design and statistical models, Archaeometry, 41, 339–364, 1999.

Gazel, E., Plank, T., Forsyth, D. W., Bendersky, C., Lee, C. A., and Hauri, E. H.: Lithosphere versus asthenosphere mantle sources at the Big Pine Volcanic Field, California, Geochemistry, Geophysics, Geosystems, 13, 2012.

Guérin, G., Mercier, N., and Adamiec, G.: Dose-rate conversion factors: update, Ancient Tl, 29, 5–8, 2011.

Heineke, C., Niedermann, S., Hetzel, R., and Akal, C.: Surface exposure dating of Holocene basalt flows and cinder cones in the Kula volcanic field (Western Turkey) using cosmogenic 3He and 10Be, Quat. Geochronol., 34, 81–91, 2016.

Huntley, D. J. and Baril, M. R.: The K content of the K-feldspars being measured in optical dating or in thermoluminescence dating, Ancient Tl, 15, 11–13, 1997.

Huntley, D. J. and Lamothe, M.: Ubiquity of anomalous fading in K-feldspars and the measurement and correction for it in optical dating, Can. J. Earth Sci., 38, 1093–1106, 2001.

Liritzis, I., Stamoulis, K., Papachristodoulou, C., and Ioannides, K.: A re-evaluation of radiation dose-rate conversion factors, Mediterranean Archaeology and Archaeometry, 13, 1–15, 2013.

Louie, J. N. and Ruprecht, P.: The blast, the quake, and the bomb: A guide to high-energy events in western Nevada, USA, 2021.

Madeira, J., Monge Soares, A. M., Brum da Silveira, A., and Serralheiro, A.: Radiocarbon dating recent volcanic activity on Faial Island (Azores), 1995.

https://doi.org/10.5194/egusphere-2026-4195
Preprint. Discussion started: 17 August 2026

McDougall, I. and Harrison, T. M.: Geochronology and Thermochronology by the 40Ar/39Ar Method, Oxford University Press, 1999.

McLachlan, H. S.: Stratigraphy, Structure, and Fluid Flow at the Soda Lake Geothermal Field, western Nevada, USA, University of Nevada, Reno, 2018.

Miallier, D., Fain, J., Montret, M., Pilleyre, T., Sanzelle, S., and Soumana, S.: Properties of the red TL peak of quartz relevant to thermoluminescence dating, Int. J. Rad. Appl. Instrum. D, 18, 89–94, 1991.

Morrison, R. B.: Lake Lahontan: geology of southern Carson desert, Nevada, US Government Printing Office, 1964.

Murray, A. S. and Wintle, A. G.: Luminescence dating of quartz using an improved single-aliquot regenerative-dose protocol, Radiat. Meas., 32, 57–73, 2000.

Murray, A. S. and Wintle, A. G.: The single aliquot regenerative dose protocol: potential for improvements in reliability, Radiat. Meas., 37, 377–381, 2003.

Oldow, J. S. and Craig, S. D.: Late Cenozoic displacement partitioning in the northwestern Great Basin, in: Geological Society of Nevada Walker Lane symposium: Structure, tectonics and mineralization of the Walker Lane: Reno, Geological Society of Nevada, 17–52, 1992.

Olmsted, F. H., Welch, A. H., Van Denburgh, A. S., and Ingebritsen, S. E.: Geohydrology, aqueous geochemistry, and thermal regime of the Soda Lakes and Upsal Hogback geothermal systems, Churchill County, Nevada, US Geological Survey, 1984.

Pilleyre, T., Montret, M., Fain, J., Miallier, D., and Sanzelle, S.: Attempts at dating ancient volcanoes using the red TL of quartz, Quat. Sci. Rev., 11, 13–17, 1992.

Prescott, J. R. and Hutton, J. T.: Cosmic ray contributions to dose rates for luminescence and ESR dating: large depths and long-term time variations, Radiat. Meas., 23, 497–500, 1994.

Preusser, F., Rufer, D., and Schreurs, G.: Direct dating of Quaternary phreatic maar eruptions by luminescence methods, Geology, 39, 1135–1138, 2011.

Reimann, T. and Tsukamoto, S.: Dating the recent past (<500 years) by post-IR IRSL feldspar – Examples from the North Sea and Baltic Sea coast, Quat. Geochronol., 10, 180–187, https://doi.org/10.1016/J.QUAGEO.2012.04.011, 2012.

Rodrigues, K., Huot, S., and Keen-Zebert, A.: Exploring the application of blue and red thermoluminescence for dating volcanic glasses, Radiat. Meas., 153, 106731, 2022a.

Rodrigues, K., Huot, S., and Keen-Zebert, A.: Exploring the application of blue and red thermoluminescence for dating volcanic glasses, Radiat. Meas., 153, 106731, 2022b.

Rosen, M. R., Reidy, L., Starratt, S., and Zimmerman, S. R. H.: Middle Holocene Hydrologic Changes Catalyzed by River Avulsion in Big Soda Lake, Nevada, USA, in: Limnogeology: Progress, Challenges and Opportunities : A Tribute to Elizabeth Gierlowski-Kordesch, edited by: Rosen, M. R., Finkelstein, D. B., Park Boush, L., and Pla-Pueyo, S., Springer International Publishing, Cham, 295–328, https://doi.org/10.1007/978-3-030-66576-0_10, 2021.

Rufer, D., Gnos, E., Mettier, R., Preusser, F., and Schreurs, G.: Proposing new approaches for dating young volcanic eruptions by luminescence methods, Geochronometria, 39, 48–56, 2012.

Russell, I. C.: Geological history of Lake Lahontan: a Quaternary lake of northwestern Nevada, U.S. Geological Survey, Washington, D.C., 288 pp., 1885.

Schmidt, C., Schaarschmidt, M., Kolb, T., Büchel, G., Richter, D., and Zöller, L.: Luminescence dating of late Pleistocene eruptions in the Eifel volcanic field, Germany, J. Quat. Sci., 32, 628–638, 2017a.

Schmidt, C., Tchouankoue, J. P., Nkouamen Nemzoue, P. N., Ayaba, F., Nformidah-Ndah, S. S., and Nformi Chifu, E.: New thermoluminescence age estimates for the Nyos maar eruption (Cameroon Volcanic Line), PLoS One, 12, e0178545, 2017b.

Smedley, R. K., Buylaert, J.-P., and Újvári, G.: Comparing the accuracy and precision of luminescence ages for partially-bleached sediments using single grains of K-feldspar and quartz, Quat. Geochronol., 53, 101007, 2019.

Sun, C., Liu, J., Xu, B., and You, H.: First radiocarbon dating of a Holocene eruption of the Datong volcanic field, eastern China, Journal of Volcanology and Geothermal Research, 384, 275–279, 2019.

Swift, D. A., Sanderson, D. C. W., Nienow, P. W., Bingham, R. G., and Cochrane, I. C.: Anomalous luminescence of subglacial sediment at Haut Glacier d'Arolla, Switzerland–a consequence of resetting at the glacier bed?, Boreas, 40, 446–458, 2011.

Team, D.: GEOROC Compilation: Minerals, https://doi.org/doi:10.25625/SGFTFN, 2024.

Thomsen, K. J., Murray, A. S., Jain, M., and Bøtter-Jensen, L.: Laboratory fading rates of various luminescence signals from feldspar-rich sediment extracts, Radiat. Meas., 43, 1474–1486, 2008.

Toyoda, S., Rink, W. J., Schwarcz, H. P., and Rees-Jones, J.: Crushing effects on TL and OSL on quartz: relevance to fault dating, Radiat. Meas., 32, 667–672, 2000.

Toyoda, S., Tsukamoto, S., Hameau, S., Usui, H., and Suzuki, T.: Dating of Japanese Quaternary tephras by ESR and luminescence methods, Quat. Geochronol., 1, 320–326, 2006.

Tsukamoto, S., Murray, A. S., Huot, S., Watanuki, T., Denby, P. M., and Bøtter-Jensen, L.: Luminescence property of volcanic quartz and the use of red isothermal TL for dating tephras, Radiat. Meas., 42, 190–197, 2007.

Tsukamoto, S., Kataoka, K. S., and Miyabuchi, Y.: Luminescence dating of volcanogenic outburst flood sediments from Aso volcano and tephric loess deposits, southwest Japan, Geochronometria, 40, 294–303, 2013.

Tsukamoto, S., Kataoka, K., Oguchi, T., Murray, A. S., and Komatsu, G.: Luminescence dating of scoria fall and lahar deposits from Somma–Vesuvius, Italy, Quat. Geochronol., 20, 39–50, 2014.

Wallinga, J., Murray, A., and Wintle, A.: The single-aliquot regenerative-dose (SAR) protocol applied to coarse-grain feldspar, Radiat. Meas., 32, 529–533, 2000.

Wintle, A. G.: Anomalous fading of thermo-luminescence in mineral samples, Nature, 245, 143–144, 1973.

Yang, H. L., Chen, J., Yao, L., Liu, C. R., Shimamoto, T., and Jobe, J. A. T.: Resetting of OSL/TL/ESR signals by frictional heating in experimentally sheared quartz gouge at seismic slip rates, Quat. Geochronol., 49, 52–56, 2019.

Zaretskaya, N. E., Ponomareva, V. V, and Sulerzhitsky, L. D.: Radiocarbon dating of large Holocene volcanic events within south Kamchatka (Russian Far East), Radiocarbon, 49, 1065–1078, 2007.

Zöller, L., Blanchard, H., and McCammon, C.: Can temperature assisted hydrostatic pressure reset the ambient TL of rocks?– A note on the TL of partially heated country rock from volcanic eruptions, Ancient TL, 27, 15–22, 2009.